

Contents lists available at ScienceDirect

# Colloids and Surfaces A: Physicochemical and Engineering Aspects

journal homepage: www.elsevier.com/locate/colsurfa



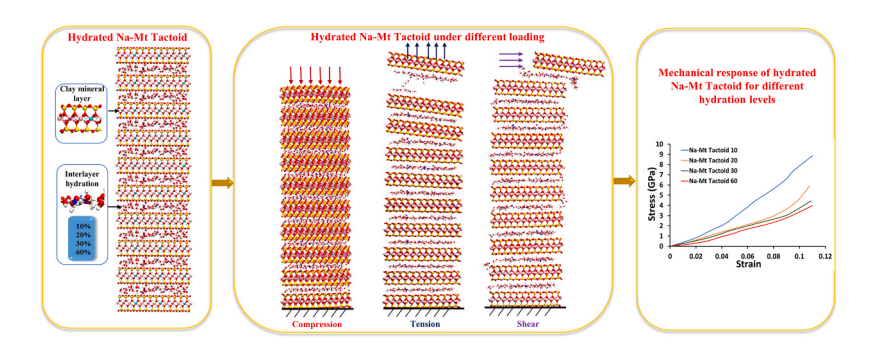


## In-silico investigation of mechanical behavior of hydrated Na-montmorillonite tactoid

H.M. Nasrullah Faisal, Hanmant K. Gaikwad, Kalpana S. Katti, Dinesh R. Katti

Department of Civil, Construction and Environmental Engineering, North Dakota State University, Fargo, ND, 58108, United States

G R A P H I C A L A B S T R A C T



#### ARTICLE INFO

Keywords: Clay Swelling Tactoid Molecular dynamics Tension Compression Shear

#### ABSTRACT

Swelling clay minerals, exemplified by Na-montmorillonite (Na-Mt), are vital constituents in expansive soils and hold significant relevance in geotechnical engineering. Comprehending their distinctive swelling behavior upon hydration is imperative for managing potential damage to civil infrastructure. Conversely, this swelling property gives rise to numerous advantageous applications, including using these clays in barrier materials and nanocomposites. The hierarchical structure of montmorillonite, consisting of clay mineral layers, tactoids, aggregates, and assemblies of aggregates, plays a pivotal role in the swelling behavior of expansive clays. This investigation employs molecular dynamics (MD) and steered molecular dynamic (SMD) simulations to explore the nanomechanical properties of hydrated Na-Mt tactoids at various hydration levels. It provides insights into their responses to compression, tensile, and shear deformation. This study reveals increased hydration levels increase interlayer spacing in clay structures, resulting in higher average d-values. Water molecules drive attractive electrostatic interactions with clay mineral layers, predominantly mediated by sodium ions, highlighting the complex interplay between interlayer hydration and tactoid stability. Higher hydration enhances tactoid compressibility, reducing the stress required for deformation by compressing water molecules and clay mineral layers in the interlayer space. The study also demonstrates a notable reduction in tensile modulus with increasing hydration, signifying the significant impact of even minimal hydration on interlayer cation-clay layer interactions. Hydrated tactoids exhibit altered mechanical responses in shear deformation compared to dry ones, requiring lower shear stress to detach the top clay layer from the tactoid. The presence of water molecules impedes the locking of clay mineral layers, further influencing mechanical properties. The results and insight

E-mail address: Dinesh.Katti@ndsu.edu (D.R. Katti).

<sup>\*</sup> Corresponding author.

provided by this work will contribute to a better understanding of the impact of interlayer hydration on the stability and response of swelling clay minerals.

#### 1. Introduction

Swelling clay mineral, an integral component of expansive soil, has long been investigated due to its unique swelling behavior upon hydration. When hydrated, swelling clay applies swelling pressure to civil infrastructures, resulting in the damage of buildings, dams, bridges, etc. [1]. Swelling clays are found all over the United States and cause an average annual damage cost of 9 billion USD [2]. Swelling clays are extensively used as landfill liners due to their high specific surface area, and low permeability [3]. Besides the geotechnical prospect, swelling clays find applications in polymer clay nanocomposites, the pharmaceutical industry, the biomedical field, and the cosmetic industries [4,5]. The swelling behavior of clays is heavily exploited in all these applications.

Na-montmorillonite (Na-Mt) is one of the most commonly found swelling clay minerals that belong to the smectite group. Na-Mt is a 2:1 phyllosilicate mineral comprising two silica tetrahedral sheets and one alumina octahedral sheet [6,7]. The clay mineral layers get negatively charged due to the isomorphous substitution of ions in the octahedral layer compensated by interlayer cations [8]. The clay interlayer properties vary significantly based on the interlayer cations. Na-Mt clay consists of a hierarchical structure at the molecular level [9]. A series of experimental studies exploring clay porosities, clay-rich soil hydration, and hydration sites confirmed the multiscale structure of clays [9-15]. The hierarchical clay structure contains a clay unit layer (t-o-t sheet), tactoid (particle containing several clay mineral layers stacked in a vertical direction), aggregate (several tactoids gathered in random orientation), and multi-aggregate (several aggregates gathered). This multiscale structure houses three layers of porosities, i.e., interlayer porosity (within tactoid), inter-tactoid porosity (within aggregate), and inter-aggregate porosity (within multi-aggregate). During clay hydration, clay interlayers contain 86 % water while other porosities contain 14 % water [13]. Therefore, investigating interlayer hydration behavior carries great important to better explain clay hydration at the molecular

Na-Mt tactoid is the basic clay particle that contains interlayer porosities. Ten identical clay mineral layers are vertically aligned to form a tactoid. The clay mineral layers of tactoid interact with each other and with interlayer cations [9]. The nanomechanical properties of tactoid significantly depend on interlayer properties. Both experimental and modeling studies showed that clay interlayer spacing increases with increasing hydration [16,17]. This is particularly relevant in swelling clays, where interlayer cation hydration leads to crystalline swelling in the interlayer space [18]. Additionally, saturated swelling clays experience the breakdown of their particles into smaller sizes, resulting in increased swelling and reduced swelling pressure [19]. This phenomenon is further studied using discrete element modeling to understand the role of particle subdivision in swelling and swelling pressure [20]. Consequently, it is essential to investigate the impact of increased interlayer hydration on tactoid interaction and mechanical behavior to bridge the swelling behavior between nano and micro scale. Molecular dynamics simulations offer a valuable approach for investigating these aspects.

Molecular dynamics (MD) simulation is a computational technique that utilizes molecular mechanics to determine the conformation and dynamics of a molecular system. The atoms are treated as classical spheres, while the bonds are treated as springs. A force field is used to compute the energy of the system [21]. Steered molecular dynamics (SMD) can be employed to investigate the mechanical response of a molecular system [22]. Both MD and SMD simulations have been employed to investigate different materials systems, including oil shale,

proteins, coronaviruses, polymer clay nanocomposites etc [9,23-32]. Different properties of clay minerals under various environmental conditions have been extensively explored using MD simulations [33-47]. Numerous MD studies have explored the hydration mechanism of clay minerals, investigating changes in counterions, interlayer water levels, and the effects of relative humidity and adsorption and transport of CO<sub>2</sub> and CH<sub>4</sub> in swelling clay systems [48–52]. However, these studies primarily focused on the clay bi-layer systems without taking into consideration the clay hierarchical structure (tactoid, aggregate etc.). In a prior study, the behavior of the dry Na-Mt clay tactoid was inspected using both MD and SMD simulations [9]. The present study addresses the clay tactoid behavior and mechanical properties in hydrated conditions. Na-Mt clay properties are determined for four different amounts of interlayer hydration, i.e., 10 %, 20 %, 30 %, and 60 % (by weight). This study probes the key mechanisms that changes the clay tactoid d-value, interlayer interactions, and deformation behavior in tactoid due to compression, tension and shear with increasing hydration.

#### 2. Methodology

#### 2.1. Model construction

The molecular model of Na-Mt tactoid has been obtained from the previous study [9]. The unit clay layer of Na-Mt was built based on Swy-2 clay with the simplified structural formula of NaSi<sub>16</sub>(Al<sub>6</sub>FeMg)  $O_{20}(OH)_4$  [41]. The utilized clay model is  $6 \times 3$  unit cells long in the XY direction with the unit cell dimensions of 5.28 Å  $\times$  9.14 Å  $\times$  6.56 Å. As the isomorphous substitution of octahedral cations produces a charge of -0.5e per unit cell, nine interlayer Na cations are placed in the interlayer. A tactoid model is built by vertically placing tenclay mineral layers on each other. The ten clay mineral layers are called B, C, D, E, F, G, H, I, J, and K from bottom to top, respectively (Fig. 1). The distance between the bottom and top clay layer is termed the "aggregated d-value". This tactoid contains nine interlayers, each of which houses nine interlayer cations. Then, water molecules are placed in each interlayer for 10 %, 20 %, 30 %, and 60 % interlayer hydration (by weight) (Fig. 2). In subsequent sections, the tactoid models with 10 %, 20 %, 30 %, and 60 % hydration levels are mentioned as Na-Mt tactoid 10, Na-Mt tactoid 20, Na-Mt tactoid 30, and Na-Mt tactoid 60, respectively. The total number of water molecules corresponding to 10 %, 20 %, 30 %, and 60 % (by weight) hydration is 72, 144, 216, and 432, respectively. The water molecules are represented by the TIP3P (Transferable Intermolecular Potential 3 Point) model. With increasing amounts of hydration, the initial dimension of the tactoid changes only in the Z-direction. The initial size of dry tactoid is 31.68 Å  $\times$  27.44 Å  $\times$ 96.56 Å. The initial size of hydrated tactoids remains the same in XY directions. The vertical height of 10 %, 20 %, 30 %, and 60 % hydrated tactoids are 114.56 Å, 132.56 Å, 168.56 Å, and 249.56 Å. The initial magnitude of aggregated d-value for 10 %, 20 %, 30 %, and 60 % hydrated tactoid are 108 Å, 126 Å, 162 Å, and 243 Å, respectively (Fig. 2). Materials Studio 7.0 was used to construct the clay model, and VMD 1.9.3 was used to add the TIP3P water molecules. CHARMm force field is utilized to parameterize the clay tactoid model, and the parameters are taken from the literature [42,53,54]. These clay parameters are consistent with other clay force field parameters [9,55]. Previous studies have also extensively validated the clay parameters with respect to the experimental results [42,56,57].

### 2.2. Simulation details

The current study performs the MD and SMD simulations of hydrated

tactoids with four different amounts of interlayer hydration (10 %, 20 %, 30 %, and 60 % by weight). The NAMD simulation package was used to perform all the MD and SMD simulations [58]. The Theoretical and Computational Biophysics Group developed NAMD in the Beckman Institute for Advanced Science and Technology at the University of Illinois at Urbana-Champaign. The MD simulations are performed to minimize and equilibrate the hydrated tactoid models. The minimization was performed at the vacuum condition using the conjugate gradient method, and then the models were brought to normal temperature (300 K) and pressure (1.01325 bar) conditions. The temperature was first raised from 0 K to 300 K in three steps with an increment of 100 K, and next, the pressure was increased from 0 bar to 1.01325 bar in four steps with 0.25 bar steps. Then, all the models are equilibrated at NTP (normal temperature and pressure) conditions for two ns with a timestep of 0.5 fs. MD simulations of hydrated clay tactoids consistently utilized periodic boundary conditions (PBC) to incorporate the Particle Mesh Ewald (PME) method for handling electrostatic interactions. The switch and cut-off distances used for van der Waals and electrostatic force calculations were 16 Å and 17 Å, respectively.

The SMD simulations were performed on equilibrated hydrated tactoids to explore clay tactoids' compression, tension and shear behavior with increasing interlayer hydration. Constant velocity SMD was employed where constant velocity was applied on the top clay layer while the bottom clay layer was fixed. The constant velocity parameters (k = 9 kcal/mol/Ų and v = 2 Å/ps) have been obtained from the previous study. To investigate the compression behavior, compressive forces were exerted on the oxygen atom from the top clay mineral layer

(K) along the Z-axis while the bottom layer (B) was fixed. The evaluation of tensile properties involved pulling the top layers vertically (forces are applied on one layer (K), two layers (J, K), three layers (I, J, K), four layers (H, I, J, K), and five layers (G, H, I, J, K) in the vertical direction) while keeping the bottom layer (B) fixed. For shear deformation, forces were applied to the surface of the top clay mineral layer (K) along the X-axis, with the bottom clay mineral layer (B) remaining fixed. The simulations were run on the Center for Computationally Assisted Science and Technology (CCAST), a North Dakota State University parallel computing facility.

#### 3. Result and discussion

# 3.1. Effect of interlayer hydration on the nanomechanical behavior and interactions in clay tactoid

The hydrated Na-Mt tactoid is analyzed for different percentages of water content. The average d-values of the equilibrated structure of Na-Mt Tactoid with 10 %, 20 %, 30 %, and 60 % water content were 13. 11 Å, 14.45 Å, 16.04 Å, and 19.95 Å respectively. In MD simulation, the average d-values are computed by finding the average spacing in the z-direction between the corresponding oxygen atoms on the clay mineral layers' surface (Table 1). Here, the average d-values of the equilibrated hydrated tactoid structure were consistent with previously reported d-values from experimental and modeling studies utilizing CHARMm forcefield and TIP3P water models to investigate clay-fluid interactions in swelling clays [16,43,46,59]. The d-values from our prior

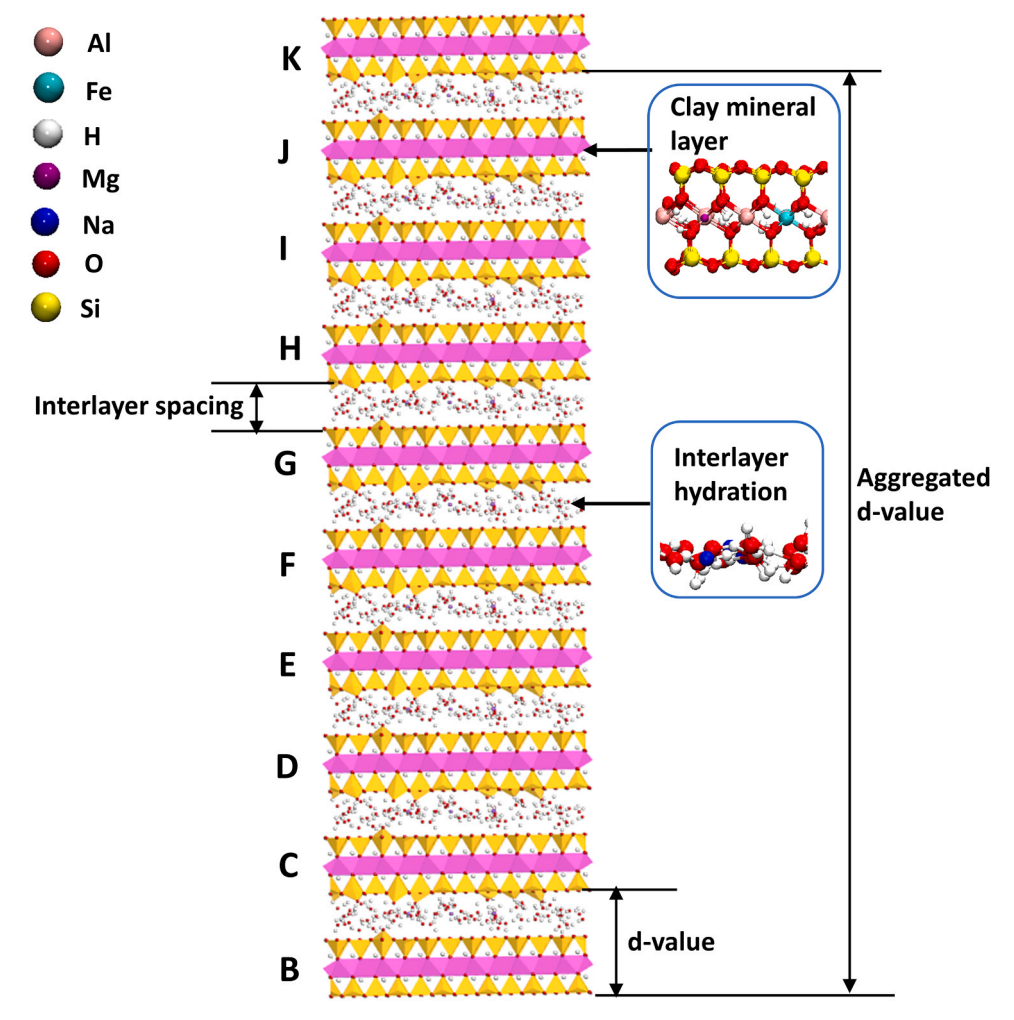


Fig. 1. Molecular model of hydrated Na-Mt tactoid containing ten clay mineral layers from B (Bottom layer) to K (top layer) with interlayer hydration.

investigation [54] for the bilayer clay model utilizing CHARMm force-field and TIP3P water model closely matched basal spacings obtained from studies for the bilayer clay model employing ClayFF and SPC water models [52,60–62] across different hydration levels (Table 1S). Furthermore, the average d-valuesobserved for ten-layer clay tactoids hydrated at 10 %, 20 %, and 30 % show a minimal deviation compared to basal spacings for the bilayer clay model evaluated in earlier studies utilizing ClayFF and SPC water models (Table 1S) [52,60–62]. In this work, the presence of water molecules promotes the expansion of the interlayer spacing within the clay structure. The interlayer spacing expanded as the hydration level increased, resulting in higher average d-values. Furthermore, increasing hydration and average d-values directly impacted the aggregated d-values. The aggregated d-values of 10 %, 20 %, 60 %, and 30 % hydrated Na-Mt tactoids are 118.05 Å, 129.60 Å, 144.47 Å, and 179.32 Å, respectively.

In the hydrated tactoid structure, water in the interlayer space leads to nonbonded interactions involving the clay mineral layers and Na ions within the interlayer. These nonbonded interactions are primarily electrostatic and Van der Waals in nature. To evaluate these interactions, we computed the interaction energies among different components such as tactoid (all clay mineral layers with Na ions), clay mineral layers, Na ions, and water in the 10 %, 20 %, 30 %, and 60 % interlayer hydrated tactoids, as shown in Table 2. Negative interaction energies indicate attractive interactions, mainly when they are predominantly electrostatic in nature, while positive values indicate repulsive interactions. Within the hydrated Na-Mt tactoid, the interaction between the tactoid and water increased with higher water content in the interlayer space. Electrostatic forces primarily drove this interaction. Notably, Na ions played a dominant role in the interaction between the tactoid and water, surpassing the contribution of the clay

**Table 1** Equilibrated d-values for hydrated Na-Mt tactoid with different hydration levels (10 %, 20 %, 30 %, and 60 %).

Clay layers	Na-Mt Tactoid 10 d-value (Å)	Na-Mt Tactoid 20 d-value (Å)	Na-Mt Tactoid 30 d-value (Å)	Na-Mt Tactoid 60 d-value (Å)
BC	13.09	14.37	16.02	19.92
CD	13.12	14.39	16.03	19.89
DE	13.12	14.65	16.05	19.97
EF	13.09	14.45	16.02	19.95
FG	13.14	14.43	16.06	19.96
GH	13.12	14.36	15.99	19.94
HI	13.09	14.37	16.05	19.97
IJ	13.12	14.52	16.12	19.96
JK	13.13	14.50	16.05	19.99
Average	13.11	14.45	16.04	19.95

mineral layers. In the 10 % interlayer hydrated tactoid, out of a total interaction energy of  $-49,394\,kJ/mol,\,-42,082\,kcal/mol$  originated from Na-water interaction, while the remaining  $-7312\,kJ/mol$  came from clay sheet-water interaction. This trend of Na ions being more influential than clay mineral layers in the tactoid-water interaction persisted as the water content increased. Similar interaction behavior was observed in higher hydration levels within the Na-Mt tactoid. The Na-water interaction and clay sheet-water interaction remained attractive in nature. As hydration increased, the attractive interaction between the clay mineral layers and water intensified due to a larger number of water molecules interacting with the clay surface. The total clay sheet-water interaction energy for the 10 % hydration tactoid was  $-7312\,kcJ/mol$ , which increased to  $-30,917\,kJ/mol$  for the 60 % hydration

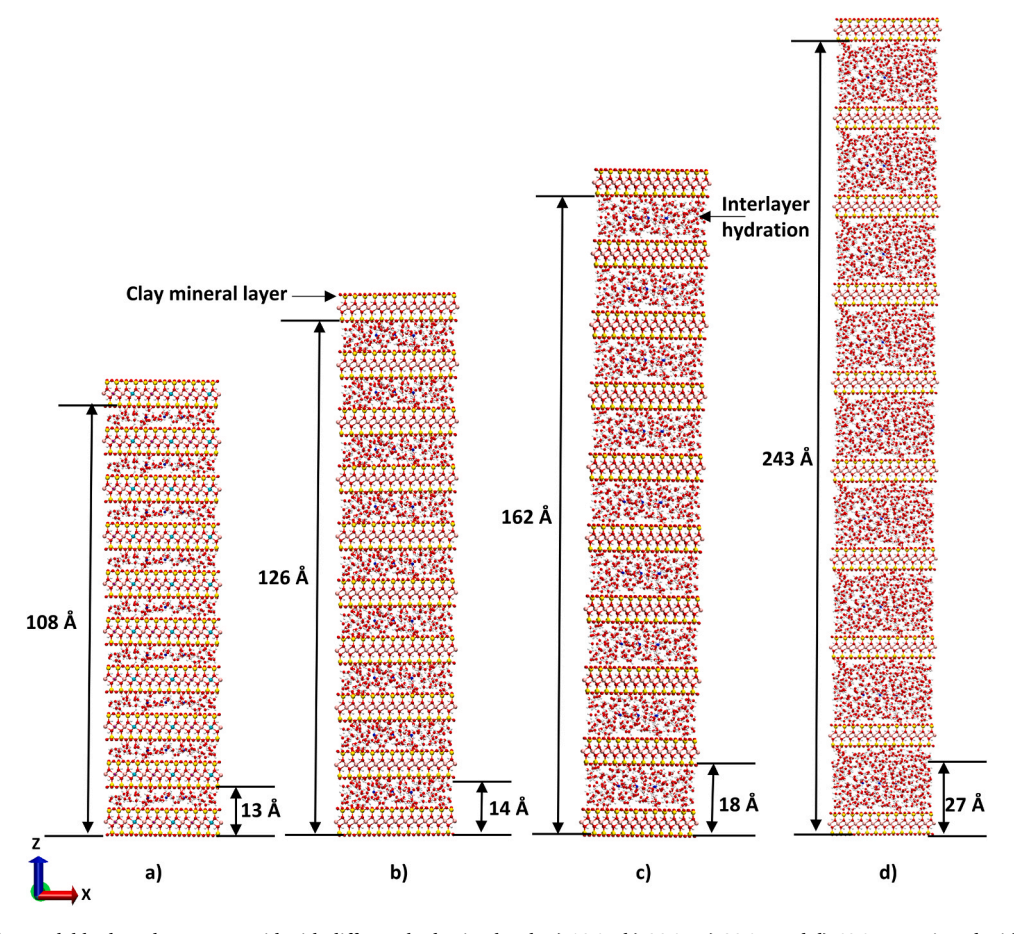


Fig. 2. Initial molecular model hydrated Na-Mt tactoid with different hydration levels a) 10 %, b) 20 %, c) 30 %, and d) 60 %, mentioned with initial d-spacing and aggregate values.

Table 2

The nonbonded interaction energies between Tactoid-water, Na-Water, Clay mineral layers-water, and Na-clay mineral layers for hydrated Na-Mt tactoid with different hydration levels (10 %, 20 %, 30 %, and 60 %). Negative and positive values of energy represent attractive and repulsive interactions, respectively.

Tactoid Models	Nonbonded Interactions between	Electrostatic (kJ/mol)	Van der Waals (VDW) (kJ/mol)	Interaction energies (kJ/mol)
Na-Mt Tactoid 10	Tactoid-water	-45137	-4256	-49394
	Na-Water	-44592	+2510	-42082
	Clay mineral layers-water	-545	-6766	-7312
	Na-clay mineral layers	-43223	-649	-43872
Na-Mt Tactoid 20	Tactoid-water	-67705	-9537	-77242
	Na-Water	-61246	+2730	-58516
	Clay mineral layers-water	-6458	-12267	-18725
	Na-clay mineral layers	-39697	-546	-40244
Na-Mt Tactoid 30	Tactoid-water	-76345	-11476	-87822
	Na-Water	-68421	+2723	-65698
	Clay mineral layers-water	-7924	-14199	-22123
	Na-clay mineral layers	-35948	-470	-36418
Na-Mt Tactoid 60	Tactoid-water	-95410	-14413	-109823
	Na-Water	-81102	+2196	-78906
	Clay mineral layers-water	-14308	-16609	-30917
	Na-clay mineral layers	-26530	-239	-26770

tactoid. Meanwhile, the Na-clay sheet interaction energy decreased from  $-43,872~\rm kJ/mol$  to  $-26,770~\rm kJ/mol$ . Previous studies have indicated that the Na-clay sheet interaction is vital for maintaining the stacked structure of the tactoid. However, with increasing hydration, the strengthened attractive interactions between Na-water and clay sheetwater reduced the attractive interaction between the clay mineral layers and Na ions, which hold the stacked structure together. This finding aligns with observations from prior studies [17,18,43]. The increased attractive interaction between water molecules and the clay mineral layers competes with the attractive energy between the clay mineral layers and Na ions, thereby impacting the stability of the stacked structure.

With increasing hydration levels, we observed reduced interaction between the clay mineral layers (layer J and layer K) in the Na-Mt tactoid. Table 3 provides a detailed account of the interactions for various components within the interlayer space. Specifically, we examined the interactions between layer J and layer K, their interactions with water molecules and Na ions within the same interlayer space, and the interactions between Na ions and water. In this interlayer space, the interaction between Na ions and water increased with hydration, influencing the interaction between Na ions and the clay mineral layers (K and J). For the 10 % hydrated Na-Mt tactoid, the interaction between Na ions and water was  $-4496~{\rm kJ/mol}$ , which increased to  $-9763~{\rm kJ/mol}$  for the 60 % hydration level. Meanwhile, the interaction between Na ions and the clay mineral layers (K and J) in the 10 % hydrated Na-Mt tactoid was  $-4980~{\rm kJ/mol}$ , but it reduced to  $-2859~{\rm kJ/mol}$  for the 60 % hydrated Na-Mt tactoid. The increase in the hydration level in the

interlayer space of the clay layer led to a decrease in the attractive interaction between Na ions and the clay mineral layers, limiting the stacking of the sheets together. Simultaneously, the presence of water in the interlayer space also impacted the interaction between the clay mineral layers (layers K and J). In previous dry tactoid studies, the interaction between layers K and J was predominantly Van der Waals in nature and measured -1842 kJ/mol [9]. However, even at 10 % hydration, this interaction drastically reduced to −652 kJ/mol. As the hydration level increased, the interaction between the clay mineral layers became repulsive and predominantly electrostatic. For the 20 %, 30 %, and 60 % hydrated tactoids, the interaction between the clay mineral layers (J and K) were +124 kJ/mol, +191 kJ/mol, and +367 kJ/mol, respectively. These changes in the interaction between the clay mineral layers had significant consequences, disrupting the stacked structure of the clay mineral layers in the Na-Mt tactoid. This is consistent with prior research on interlayer swelling, where water molecules enter the interlayer space, causing individual clay mineral layers to disperse, leading to the particles' breakdown [17,19]. Additionally, earlier studies indicate that water activity dictates the stability of hydration states and cationic partitioning within clay minerals [62]. Variations in intercalation Gibbs free energy associated with water activity directly impact the thermodynamically stable hydrated state and significantly influence the stability and structural integrity of clay minerals [62]. In this study, the altered interaction between the clay mineral layers (layers K and J) also contributed to the disruption of the stacked structure of clay mineral layers within the tactoid. Moreover, increasing the hydration level beyond 60 % further increased the

Table 3

The nonbonded interaction energies between Layer K-layer J, Layer K and J -Water, Na-water, and Na-Layer K and J for hydrated Na-Mt tactoid with different hydration levels (10 %, 20 %, 30 %, and 60 %). Negative and positive values of energy represent attractive and repulsive interactions, respectively.

Tactoid Models	Nonbonded Interactions between	Electrostatic (kJ/mol)	Van der Waals (VDW) (kJ/mol)	Interaction energies (kJ/mol)
Na-Mt Tactoid 10	Layer K-layer J	+158	-810	-652
	Layer K and J -Water	-154	-768	-921
	Na-water	-4799	+303	-4496
	Na-Layer K and J	-4917	-62	-4980
Na-Mt Tactoid 20	Layer K-layer J	+565	-442	+124
	Layer K and J -Water	-817	-1295	-2112
	Na-water	-7506	+344	-7162
	Na-Layer K and J	-4202	+-63	-4265
Na-Mt Tactoid 30	Layer K-layer J	+400	-209	+191
	Layer K and J -Water	-1069	-1556	-2625
	Na-water	-7957	+309	-7648
	Na-Layer K and J	-3998	-44	-4042
Na-Mt Tactoid 60	Layer K-layer J	+382	-15	+367
	Layer K and J -Water	-1792	-1811	-3603
	Na-water	-10025	+261	-9763
	Na-Layer K and J	-2836	-22	-2859

repulsive interaction between the clay mineral layers. This heightened repulsion may eventually separate the clay mineral layers, ultimately leading to the breakdown of the tactoid particles.

# 3.2. Influence of hydration levels on the compression behavior of Na-Mt tactoid

This study investigated the compression response of hydrated tactoids at different hydration levels using SMD. During the compression process, external forces were applied to the surface oxygen atoms of the top clay layer (layer K), while the bottom clay layer remained fixed (Fig. 3a). Our analysis focused on the aggregated d-value of the hydrated tactoid, which significantly changed with the application of compressive stress. We observed that increasing hydration required less compressive stress to induce the same amount of deformation in the hydrated tactoid. Specifically, for the Na-Mt Tactoid 10, the aggregated d-value decreased from 118.05 Å to 103.7 Å, indicating a compression of 14.52 Å at 10.36 GPa stress. Similarly, for the Na-Mt Tactoid 20, the aggregated d-value reduced from 129.60 Å to 115.69 Å, corresponding to a compression of 13.97 Å at 5.92 GPa stress. For Na-Mt Tactoid 30, the

aggregated d-value decreased from 144.47 Å to 128.74 Å, resulting in a compression of 15.73 Å at 4.44 GPa stress, while for Na-Mt Tactoid 60, the aggregated d-value reduced from 179.32 Å to 163.46 Å, with a compression of 15.86 Å at 3.98 GPa stress. Fig. 3c demonstrates the faster decrement of the aggregated d-value for higher hydration levels of the tactoid (also refer to Figure 1S), achieved with less compressive stress. This indicates that as the hydration increases, the tactoid becomes more compressible, with water playing a significant role in this behavior. The reduction in the interlayer space during compression was mainly attributed to the decreased distance between the clay mineral layers (Fig. 3b). As reported in previous studies [3], a similar observation was made in our study where, initially, deformation occurred in the void spaces between the clay mineral layers and fluids. As compression continued, water molecules became compressed, and the clay mineral layers started to deform. However, the decrease in the spacing (thickness) of clay mineral layers was found to be insignificant during compression. Furthermore, more significant deformation was observed at the top portion of the tactoid during the compression process compared to the bottom portion. This trend continued along the hydrated tactoid, with the extent of deformation gradually decreasing from

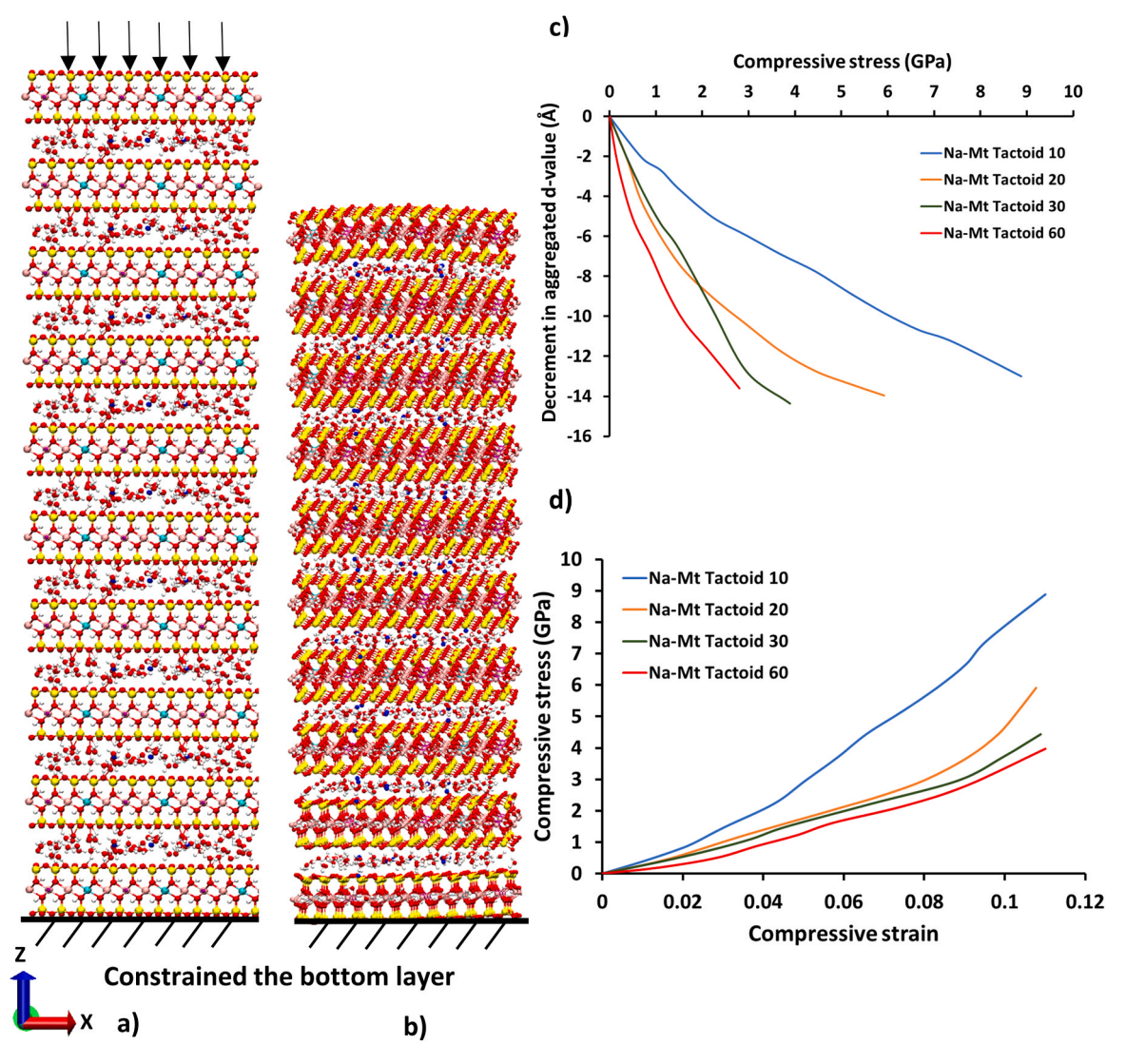


Fig. 3. Hydrated Na-Mt tactoid model under compression. a) Compression test set up where the bottom layer of equilibrated model (Na-Mt Tactoid 10) is fixed and compressive force applied at top layer using constant velocity SMD b) Compressed Na-Mt Tactoid 10 model attributed to decrease in interlayer space between clay mineral layers c) Decrement in aggregated d-value (Initial aggregated d-value minus final aggregated d-value) vs compressive stress plot hydrated tactoid models shows the faster decrement in interlayer space with less compressive stress for higher hydration level d) Compressive stress-strain response for hydrated Na-Mt tactoid for different hydration level (10 %, 20 %, 30 %, and 60 %) becomes softer as hydration increases in interlayer space.

top to bottom.

The number of water molecules present inside the interlayer space significantly influenced the compressive response of the hydrated tactoid. We observed different stress-strain behaviors in the Na-Mt tactoid by varying the hydration level. Fig. 3d shows the stress-strain response for all hydrated tactoid models, where strain values are calculated by dividing the deformation in aggregated d-values by the height of the equilibrated hydrated tactoid. Here, the stress-strain response is divided into Region I (0-0.05 strain) and Region II (0.05-0.11 strain). Deformation in region II leads to a stiffer response compared to region I. We evaluated the compression modulus for all hydrated tactoid structures in both regions using the least square method to quantify this. In region I, the compressive moduli are 52.42, 35.94, 32.17, and 28.35 GPa for Na-Mt Tactoid 10, Na-Mt Tactoid 20, Na-Mt Tactoid 30, and Na-Mt Tactoid 60, respectively. The stress-strain behavior for the ten-layer hydrated clay tactoid observed in region I is consistent with prior studies for the bilayer clay models [54,63,64], indicating a softer response (decreasing moduli) with increasing hydration. Moreover, the calculated compression moduli for ten-layer clay tactoid hydrated at 10 %, 20 %, and 30 % closely match those reported in prior studies for the bilayer clay model; where Zhao et al. predicted 48.32, 38.69, and 32.62 GPa; Xu et al. predicted 50.34, 40.83, and 38.75 GPa; Schmidt et al. predicted 30.62, 25.26, and 19.86 GPa; for 10 %, 20 %, and 30 % hydration levels, respectively [54,63,64]. In Region II, the compressive moduli are 98.31,

88.01, 52.58, and 51.17 GPa for the same tactoid models. The compressive moduli in Region II were significantly higher than those in Region I for all hydrated tactoid models. In region I, the initial deformation resulted from the compression of the void space between the clay mineral layers and water molecules, requiring less force and resulting in lower compressive moduli. In contrast, in Region II, as the void space filled, the deformation was caused by the compression of both water molecules and clay mineral layers, necessitating higher stress and resulting in higher moduli. Moreover, we also observed that as the hydration level increases, the stress-strain response becomes softer, leading to a reduction in compression moduli in both regions of the tactoid. Even with just 10 % hydration, the compression modulus for the hydrated tactoid is drastically reduced from 125.1 to 52.42 GPa compared to the dry tactoid [9] in the initial deformation stage, and this reduction continues with further increases in hydration. Here, the compression in the tactoid is not solely due to the compression of the void space between clay mineral layers and fluids but also from the compression of fluid' layers. The increase in water molecules within the interlayer space contributed to a substantial amount of compression, requiring relatively smaller magnitudes of stress. Therefore, the hydration level played a crucial role in softening the stress-strain response and reducing the overall compression moduli in both regions of the hydrated Na-Mt

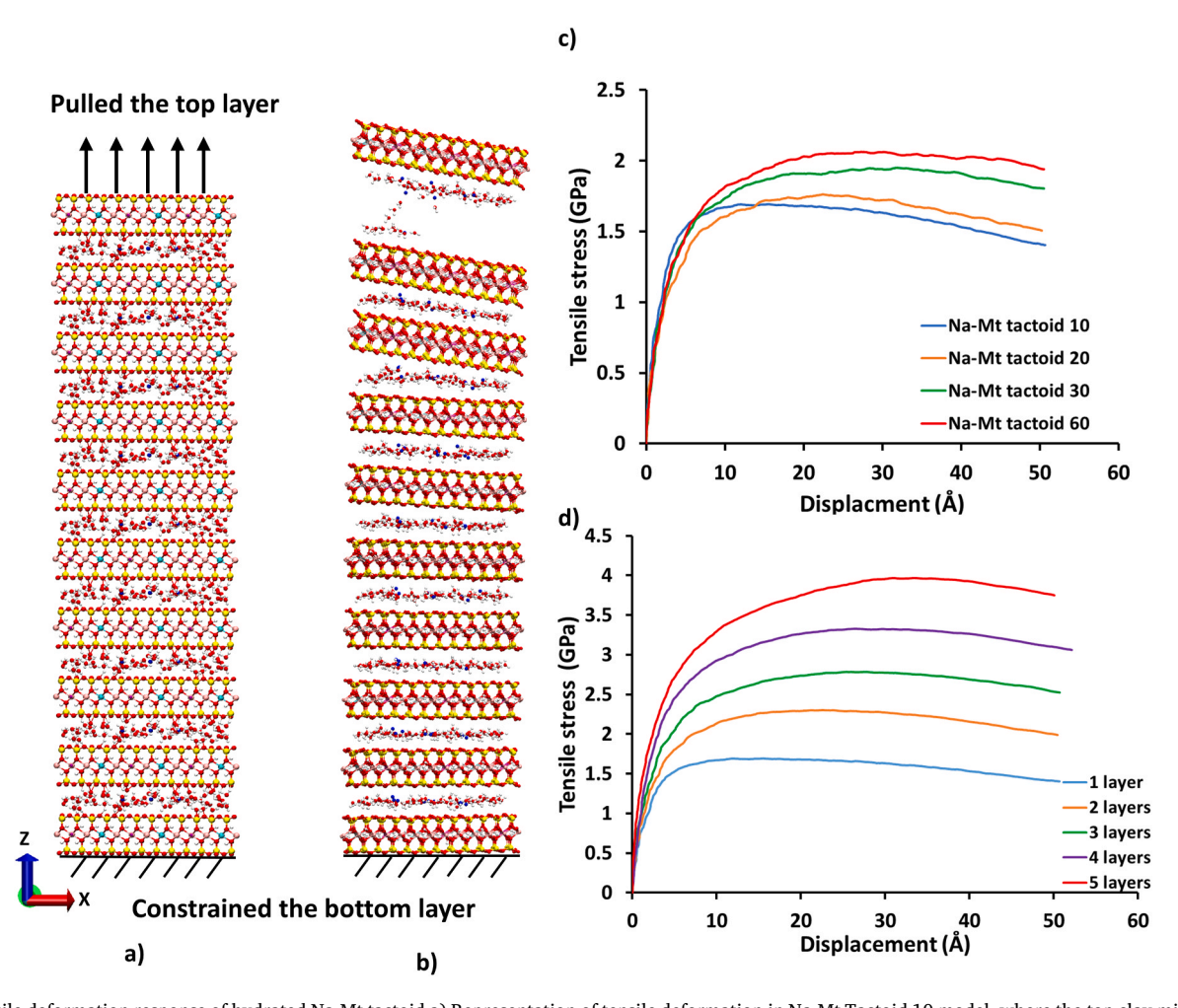
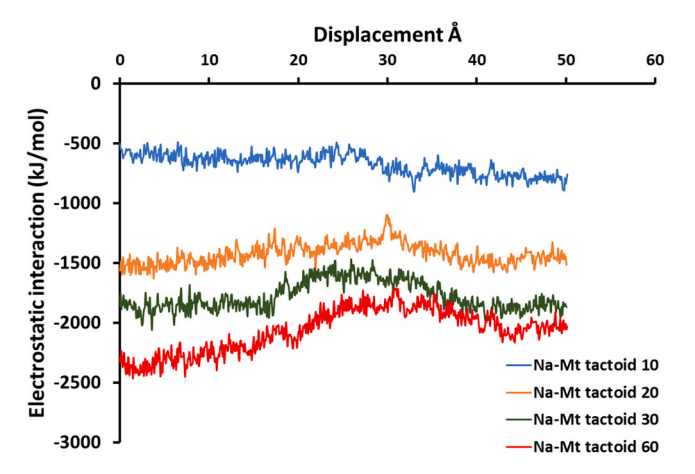


Fig. 4. Tensile deformation response of hydrated Na-Mt tactoid a) Representation of tensile deformation in Na-Mt Tactoid 10 model, where the top clay mineral layer is pulled vertically, and the bottom layer is constrained b) Tensile deformed Na-Mt Tactoid 10 model showed the attachment of water molecules to top clay mineral layer K during detachment of top layer from the rest of tactoid c) Plot of tensile stress vs displacement for hydrated Na-Mt tactoid for different hydration level (10 %, 20 %, 30 %, and 60 %) d) Tensile stress vs displacement response for Na-Mt Tactoid 10 model after pulling one (K), two (J, K), three (I, J, K), four (H, I, J, K), and five (G, H, I, J, K) top clay mineral layers.

#### 3.3. Effect of hydration on tensile deformation behavior in Na-Mt tactoid

The tensile behavior of the hydrated tactoid is investigated by pulling the top clay mineral layer of the equilibrated hydrated Na-Mt tactoid in the vertical direction (Fig. 4a). The results, presented in Table 2, reveal that as hydration levels increase between the clay mineral layers, the attraction between Na ions and clay mineral layers diminishes, impacting the stacking of the clay structure. Consequently, the influence of hydration on the tensile deformation of the Na-Mt tactoid becomes evident. The relationship between tensile stress and displacement of the top clay layer, K, is shown in the Fig. In the linear range, spanning around 4 Å, all hydrated tactoid models display a linear correlation between stress and displacement (Fig. 4c). Upon further extension up to 20 Å, a slight stress increment is observed. However, as the clay layer extends beyond this point, the required tensile stress for deforming layer K begins to decrease, indicating the detachment of the clay mineral layer from the rest of the tactoid across all models. Within the linear region, the stiffer response of hydrated tactoid decreases with increasing hydration levels. This is attributed to the reduction in interaction between Na ions and clay mineral layers K and J (Table 3), which affects the mechanical behavior of the hydrated tactoid and leads to a decrease in tensile modulus. Specifically, for hydrated tactoids at 10 %, 20 %, 30 %, and 60 % hydration levels, the observed tensile moduli are 52.43 GPa, 50.49 GPa, 48.63 GPa, and 47.31 GPa, respectively. In comparison to dry tactoid, the hydrated counterparts require less force to initiate the detachment of the top clay layer K. For instance, in the case of 10 % hydrated tactoid, a stress of 1.68 GPa is needed for this detachment, while dry tactoid requires 2.87 GPa [9]. The decreased stress also significantly impacts the mechanical properties of the 10 % hydrated tactoid, reducing the tensile modulus from 133 GPa (for dry tactoid) to 52 GPa. Here, 10 % of hydration significantly affects the interaction between interlayer cations and clay mineral layers. For Na-Mt Tactoid 10, the interaction energy between Na ions and clay mineral layers is substantially decreased from 59,738 kJ/mol to 43,872 kJ/mol compared to dry tactoid [9], and this reduction further continues as hydration increases. As a result, the diminished interaction between Na ions and clay mineral layers disrupts the stacking of clay mineral layers, decreasing the tensile modulus.

During the process of tensile deformation, we noticed that despite having a lower tensile modulus, tactoids with higher hydration levels increased maximum stress when detaching the top clay layer, K, from the tactoid structure. This phenomenon can be attributed to the attachment of water molecules to the clay mineral layer K during detachment (Fig. 4b). As hydration increased, more water molecules became attached to the top clay mineral layer K, fostering a stronger



**Fig. 5.**: The nonbonded interaction between top clay mineral K and interlayer water molecule (between layer K and layer J) shows the strong interaction as hydration increases during tensile deformation.

interaction between the water molecules and the layer K, as shown in Fig. 5. Analyzing the number of attached water molecules revealed that with higher hydration levels, a more significant number of water molecules were associated with the top mineral layer K. Specifically, out of the interlayer water molecules between layer K and J (72, 144, 216, and 432 for 10 %, 20 %, 30 %, and 60 % hydrated tactoids, respectively), 60, 107, 178, and 214 water molecules were attached to the top layer K. This attachment of water molecules to the clay layer K contributed to the augmented tensile stress observed during detachment of layer K from rest of tactoid with increased hydration levels. Simultaneously, we analyzed the tensile deformation behavior for hydrated tactoids after sequentially pulling off different numbers of layers starting from one layer (K), two layers (J, K), three layers (I, J, K), four layers (H, I, J, K), and five layers (G, H, I, J, K) in the vertical direction. With an increasing number of layers during pulling, the tensile response became progressively stiffer, demanding greater force for the complete detachment of layers from the rest of the tactoid structure, as shown in Fig. 4d. For instance, in the 10 % hydrated tactoid case, initiating the detachment of a single layer required a stress of 1.68 GPa, whereas detaching five layers required 3.87 GPa (Fig. 4d). A similar tensile behavior was also observed across the other hydrated tactoid models (Figure 2S). As the number of layers involved in the detachment increased, the nonbonded interactions between these layers and the remainder of the tactoid intensified. Additionally, the increased number of atoms being pulled in the vertical direction contributed to a greater force requirement for detaching layers from the hydrated tactoid structure.

# 3.4. Shear deformation and hydration-induced mechanical changes in Na-Mt tactoid

The hydrated Na-Mt tactoid was subjected to shearing by moving the upper clay mineral layer K horizontally while keeping the bottom layer B fixed, as shown in Fig. 6a. A constant velocity SMD of 2 Å/ps velocity was used to deform the hydrated tactoid horizontally. As shear stress was applied to the upper clay mineral layer K, it slid relative to layer J, causing slight deformation in layer J in the direction of the applied force (Fig. 6b). Importantly, unlike in the dry case [9], sliding motion was not observed for the remaining bottom clay mineral layers. This change in behavior was attributed to increasing hydration, which led to a decrease in the interaction between Na cations and the top layers K and J, as indicated in Table 3. Consequently, layer J had no corresponding movement even after clay layer K slid in the shear direction. In contrast, dry tactoids exhibited sliding of the top clay mineral layers relative to each other, with the fixed bottom layer, B, showing the least displacement [9]. This sliding of layers led to the locking of Na cations within the tetrahedral cavities of clay minerals, which in turn initiated the locking of the sliding phenomena of clay mineral layers [9,46]. However, water molecules within the interlayer space created a solvation shell surrounding the Na cations in hydrated tactoids, limiting their locking within the tetrahedral cavities. As a result, the locking phenomena observed in dry tactoids were absent in the hydrated ones, fundamentally altering the mechanical response of the hydrated tactoid.

As shear deformation continued in the hydrated tactoid, the top clay mineral layer K detached from the adjacent layer J and from the rest of the tactoid, moving approximately 30 Å in all hydrated tactoid models. Fig. 6c illustrates the shear deformation response for all models, plotting shear stress against displacement. In the initial deformation phase up to 10 Å, the shear stress required for deformation was roughly 1.5 GPa for all models (Fig. 6c). However, as the detachment approached (at 30 Å), the shear stress increased to 2.25 GPa for all models (Fig. 6c). In the initial deformation stage, the interaction between Na cations and clay mineral layers K and J resisted deformation, necessitating higher stress for shearing up to 10 Å. However, as deformation progressed, the clay layer K slid in the shear direction without locking Na cations in the tetrahedral cavities due to interlayer swelling where water surrounds the Na cations (Fig. 7). This resulted in lower stress (0.75 GPa) required

### Shear force at top layer

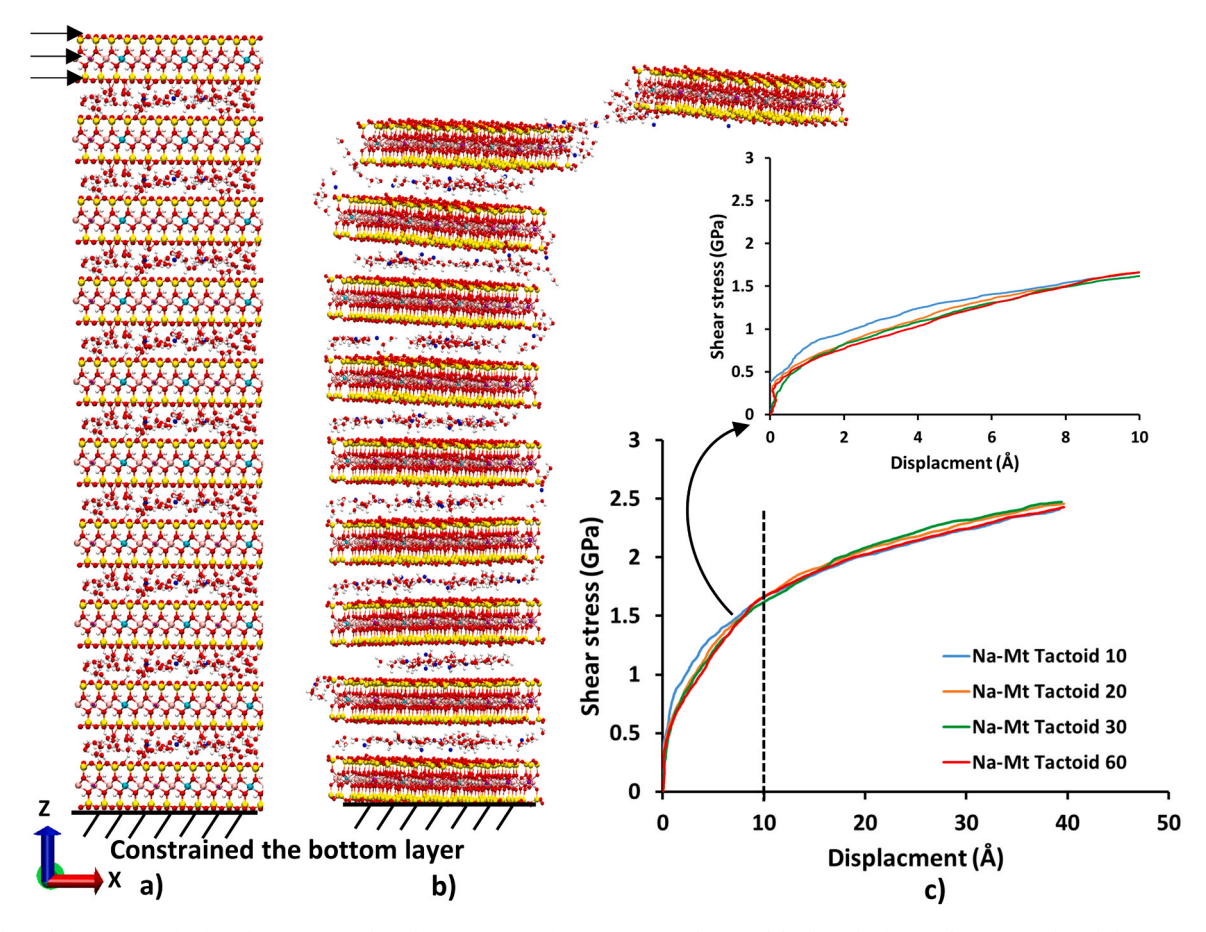


Fig. 6.: Shear deformation in hydrated Na-Mt tactoid a) Shear test set up for Na-Mt Tactoid 10 model where the bottom layer is fixed, and shear forces are on top layer b) Shearing of Na-Mt Tactoid 10 shows the sliding of top clay mineral layer on adjacent layer J c) Shear stress vs displacement plot for hydrated Na-Mt tactoid with different hydration levels (10 %, 20 %, 30 %, and 60 %).

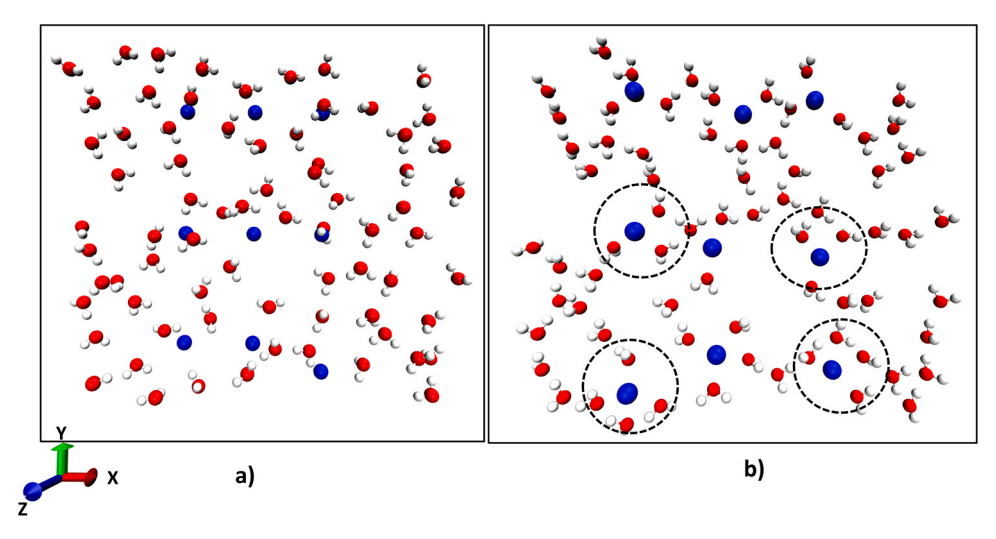


Fig. 7. Interlayer water molecules and Na cations between clay mineral layer (J) and (K) of NA-Mt Tactoid 10 model a) Initial structure b) Equilibrated structure where water molecules surround the Na cations.

for the subsequent 20 Å of deformation. In contrast, the shear deformation response in dry tactoid was divided into two phases: first, Na cations slid in the tetrahedral cavities, and second, they initiated the locking of clay mineral layers, leading to a significant increase in shear stress (up to 6.67 GPa) (Figure 3S) required for the detachment of clay

layer K from the rest of the tactoid [9]. However, increased interlayer swelling in hydrated tactoids reduced the interaction between Na cations and clay mineral layers K and J (Table 3), affecting their stacking. Additionally, the water surrounding Na cations (Fig. 7b) failed to initiate the locking of clay mineral layers, resulting in a lower force

required to detach the top clay layer. Here, increasing hydration led to reduced interactions between Na cations and clay mineral layers K and J, altering the mechanical properties of hydrated tactoids during shear deformation. This aligns with prior findings from non-equilibrium MD simulations on Arizona-type montmorillonite, where frictional weakness and velocity-strengthening behavior in shear-induced interlayer sliding were observed, indicative of aseismic slip[65]. The influence of hydrogen bond formation around cations on clay mineral hydration state significantly affects frictional behavior, resulting in diverse hydration states that impact interlayer sliding and frictional strength[65]. These variations in hydration state due to hydrogen bonding influence fault slip stability, akin to the observed effect on the locking of sliding phenomena of clay mineral layers [9,46] due to an increase in hydration during our simulation.

The shear moduli for different hydration level tactoids were evaluated in the initial deformation region (up to  $10\,\text{Å}$ ), where the deformation in the top layer transformed into shear strain after considering the height of equilibrated hydrated tactoid models. The shear moduli for  $10\,\%$ ,  $20\,\%$ ,  $30\,\%$ , and  $60\,\%$  hydrated tactoids were 25.39, 18.65, 17.98, and  $17.36\,$  GPa, respectively. Comparing these values to the dry tactoid ( $69.56\,$  GPa) [9], it's evident that even  $10\,\%$  hydration significantly reduced the shear modulus, indicating the impact of hydration on the separation of clay mineral layers during shearing. Furthermore, increasing hydration decreased the shear modulus due to the reduced interaction between Na cations and clay mineral layers. However, the interaction between water and clay mineral layers K and J increased with hydration, leading to the attachment of water molecules to the top layer K during deformation (Fig. 6b) and resulting in consistent shear stress required to detach the top layer from the tactoid.

#### 4. Conclusions

The MD and SMD study of hydrated Na-Mt tactoid provides valuable insights into the mechanical behavior at different hydration levels, particularly in response to compression, tensile, and shear deformation. This work highlights the crucial role of water molecules within the interlayer space in influencing these clay mineral assemblies structural and mechanical properties. It shows that increasing hydration levels leads to the expansion of the interlayer spacing within the tactoid structure. The presence of water molecules significantly impacted the nonbonded interactions within the tactoid, particularly between the tactoid and water, primarily driven by electrostatic forces. Notably, Na ions played a dominant role in the attractive interactions with water molecules, surpassing the contribution of the clay mineral layers. This shift in interaction dynamics became more pronounced with increasing hydration levels, ultimately affecting the stability of the stacked structure. The increased attractive interaction between water molecules and clay mineral layers competed with the attractive energy between the clay mineral layers and Na ions, potentially leading to the breakdown of the tactoid particles.

Furthermore, this study explored the compression response of hydrated tactoid, revealing that higher hydration levels made the tactoid more compressible. Water molecules played a significant role in this behavior, contributing to the reduction in interlayer spacing during compression. This reduction was mainly attributed to the compression of water molecules, while the thickness of clay mineral layers remains relatively stable. This change in hydration level also influences the stress-strain response, resulting in a softer behavior as hydration increases. During tensile deformation, even a small amount of hydration significantly affected the interaction between interlayer cations and clay mineral layers, decreasing tensile modulus. Higher hydration levels also increased the maximum stress observed during detachment due to the attachment of water molecules to the top clay layer. This attachment fostered a stronger interaction between water molecules and the clay layer, influencing the mechanical response of the hydrated tactoid. Further, in shear deformation, the interlayer swelling in hydrated

tactoids alters their mechanical response compared to dry tactoids. The detachment of the top clay layer from the rest of the tactoid requires lower shear stress in hydrated tactoid due to reduced interactions between Na ions and clay mineral layers. Additionally, the presence of water molecules inhibits the locking of clay mineral layers, further impacting the mechanical properties.

This study underscores the intricate interplay between water molecules and clay mineral layers within hydrated Na-Mt tactoids, ultimately influencing their structural and mechanical behavior. The findings and insights provided by this work not only enhance our understanding of intercalation, exfoliation, deformation behavior, and particle breakdown in swelling clays but also highlight the pivotal role of interlayer interactions in the swelling process of smectite clays.

#### CRediT authorship contribution statement

Dinesh Ramanath Katti: Writing – review & editing, Visualization, Supervision, Resources, Project administration, Methodology, Investigation, Funding acquisition, Conceptualization. Kalpana S. Katti: Writing – review & editing, Supervision, Resources, Project administration, Funding acquisition, Conceptualization. Hanmant K. Gaikwad: Writing – original draft, Validation, Software, Methodology, Formal analysis. H. M. Nasrullah Faisal: Writing – original draft, Visualization, Methodology, Investigation, Formal analysis.

#### **Declaration of Competing Interest**

The authors declare that they have no known competing financial interests or personal relationships that could have appeared to influence the work reported in this paper.

#### Data availability

Data will be made available on request.

#### Acknowledgments

This work was supported by the USDoT, Mountain Plains Consortium (MPC) grants MPC-506 (agreement #DTRT13-G-UTC38) and MPC-548 (agreement #69A3551747108). The Computationally Assisted Science and Technology (CCAST) (NSF MRI grant #1229316 and #2019077) provided the computational resources at North Dakota State University.

#### Appendix A. Supporting information

Supplementary data associated with this article can be found in the online version at doi:10.1016/j.colsurfa.2024.134117.

### References

- O. Buzzi, S. Fityus, S.W. Sloan, Use of expanding polyurethane resin to remediate expansive soil foundations, Can. Geotech. J. 47 (2010) 623–634.
- [2] J.C. Pérez, J.C. Ruge, J.P. Rojas, J.A. Orjuela, J.R. Cáceres, Experimental assessment of swelling potential in montmorillonite soils. Journal of Physics: Conference Series, IOP Publishing, 2021 012006.
- K.B. Thapa, K.S. Katti, D.R. Katti, Compression of Na–Montmorillonite swelling clay interlayer is influenced by fluid polarity: a steered molecular dynamics study. Langmuir 36 (2020) 11742–11753.
- [4] A. Ambre, K.S. Katti, D.R. Katti, In situ mineralized hydroxyapatite on amino acid modified nanoclays as novel bone biomaterials, Mater. Sci. Eng.: C 31 (2011) 1017–1029.
- [5] D.R. Katti, Z.R. Patwary, K.S. Katti, Modelling clay-fluid interactions in montmorillonite clays, Environ. Geotech. 4 (2017) 322–338.
- [6] R.E. Grim, Modern concepts of clay materials, J. Geol. 50 (1942) 225–275.
- [7] R.E. Grim, Clay Mineralogy, McGraw-Hill, New York, 1968, p. 206.
- [8] S.B. Hendricks, M.E. Jefferson, Structures of kaolin and talc-pyrophyllite hydrates and their bearing on water sorption of the clays, Am. Mineral. 23 (1938) 863–875.
- [9] H.M.N. Faisal, K.S. Katti, D.R. Katti, Molecular mechanics of the swelling clay tactoid under compression, tension and shear, Appl. Clay Sci. (2020) 105908.
- [10] L. Massat, O. Cuisinier, I. Bihannic, F. Claret, M. Pelletier, F. Masrouri, S. Gaboreau, Swelling pressure development and inter-aggregate porosity

- evolution upon hydration of a compacted swelling clay, Appl. Clay Sci. 124 (2016) 197–210.
- [11] W.J. Likos, A. Wayllace, Porosity evolution of free and confined bentonites during interlayer hydration, Clays Clay Miner. 58 (2010) 399–414.
- [12] M. Jullien, J. Raynal, E. Kohler, O. Bildstein, Physicochemical reactivity in clayrich materials: Tools for safety assessment, Oil Gas. Sci. Technol. -Rev. D. Ifp Energ. Nouv. 60 (2005) 107–120.
- [13] J.N. Perdrial, L.N. Warr, Hydration behavior of mx80 bentonite in a confined-volume system: implications for backfill design, Clays Clay Miner. 59 (2011) 640–653.
- [14] F. Salles, J.-M. Douillard, R. Denoyel, O. Bildstein, M. Jullien, I. Beurroies, H. Van, Damme, Hydration sequence of swelling clays: Evolutions of specific surface area and hydration energy, J. Colloid Interface Sci. 333 (2009) 510–522.
- [15] F. Salles, I. Beurroies, O. Bildstein, M. Jullien, J. Raynal, R. Denoyel, H. Van, Damme, A calorimetric study of mesoscopic swelling and hydration sequence in solid Na-montmorillonite, Appl. Clay Sci. 39 (2008) 186–201.
- [16] P.M. Amarasinghe, K.S. Katti, D.R. Katti, Molecular hydraulic properties of montmorillonite: a polarized fourier transform infrared spectroscopic study, Appl. Spectrosc. 62 (2008) 1303–1313.
- [17] S.M. Pradhan, K.S. Katti, D.R. Katti, Evolution of molecular interactions in the interlayer of Na-montmorillonite swelling clay with increasing hydration, Int. J. Geomech. 15 (2015).
- [18] D.R. Katti, L. Srinivasamurthy, K.S. Katti, Molecular modeling of initiation of interlayer swelling in Na-montmorillonite expansive clay, Can. Geotech. J. 52 (2015) 1385–1395.
- [19] D.R. Katti, V. Shanmugasundaram, Influence of swelling on the microstructure of expansive clays, Can. Geotech. J. 38 (2001) 175–182.
- [20] D.R. Katti, M.I. Matar, K.S. Katti, P.M. Amarasinghe, Multiscale modeling of swelling clays: a computational and experimental approach, Ksce J. Civ. Eng. 13 (2009) 243–255.
- [21] D. Young, Computational chemistry: a practical guide for applying techniques to real world problems, John Wiley & Sons, 2004.
- [22] S. Izrailev, S. Stepaniants, B. Isralewitz, D. Kosztin, H. Lu, F. Molnar, W. Wriggers, K. Schulten, Steered molecular dynamics. Computational molecular dynamics: challenges, methods, ideas, Springer, 1999, pp. 39–65.
- D.R. Katti, K. Thapa, K.S. Katti, Modeling molecular interactions of sodium montmorillonite clay with 3D kerogen models. Fuel 199 (2017) 641–652.
- [24] H.M.N. Faisal, K.S. Katti, D.R. Katti, Modeling the behavior of organic kerogen in the proximity of calcite mineral by molecular dynamics simulations, Energy Fuels 34 (2020) 2849–2860.
- [25] H.M.N. Faisal, K.S. Katti, D.R. Katti, An insight into quartz mineral interactions with kerogen in Green River oil shale, Int. J. Coal Geol. 238 (2021) 103729.
- [26] H.M.N. Faisal, K.S. Katti, D.R. Katti, Binding of SARS-COV-2 (COVID-19) and SARS-COV to human ACE2: identifying binding sites and consequences on ACE2 stiffness. Chem. Phys. 551 (2021) 111353.
- [27] H.M.N. Faisal, K.S. Katti, D.R. Katti, Differences in interactions within viral replication complexes of SARS-CoV-2 (COVID-19) and SARS-CoV coronaviruses control RNA replication ability, JOM (Warrendale, Pa.: 1989) (2021) 1–12.
- [28] S.V. Jaswandkar, H.M.N. Faisal, K.S. Katti, D.R. Katti, Dissociation mechanisms of g-actin subunits govern deformation response of actin filament, Biomacromolecules 22 (2021) 907–917.
- [29] S.V. Jaswandkar, K.S. Katti, D.R. Katti, Molecular and structural basis of actin filament severing by ADF/cofilin, Comput. Struct. Biotechnol. J. 20 (2022) 4157–4171.
- [30] H.K. Gaikwad, S.V. Jaswandkar, K.S. Katti, A. Haage, D.R. Katti, Molecular basis of conformational changes and mechanics of integrins, Philos. Trans. R. Soc. A: Math. Phys. Eng. Sci. 381 (2023) 20220243.
- [31] D. Sikdar, S.M. Pradhan, D.R. Katti, K.S. Katti, B. Mohanty, Altered phase model for polymer clay nanocomposites, Langmuir 24 (2008) 5599–5607.
- [32] R. Bhowmik, K.S. Katti, D. Venna, D.R. Katti, Probing molecular interactions in bone biomaterials: through molecular dynamics and Fourier transform infrared spectroscopy, Mater. Sci. Eng. C. -Biomim. Supramol. Syst. 27 (2007) 352–371.
- [33] A. Lloret, M.V. Villar, M. Sanchez, A. Gens, X. Pintado, E.E. Alonso, Mechanical behaviour of heavily compacted bentonite under high suction changes, Geotechnique 53 (2003) 27–40.
- [34] F.L. Pellet, M. Keshavarz, M. Boulon, Influence of humidity conditions on shear strength of clay rock discontinuities, Eng. Geol. 157 (2013) 33–38.
- [35] M.V. Villar, A. Lloret, Influence of temperature on the hydro-mechanical behaviour of a compacted bentonite, Appl. Clay Sci. 26 (2004) 337–350.
- [36] F.R.C. Chang, N.T. Skipper, G. Sposito, Computer-simulation of interlayer molecular-structure in sodium montmorillonite hydrates, Langmuir 11 (1995) 2734–2741.
- [37] S. Karaborni, B. Smit, W. Heidug, J. Urai, E. van Oort, The swelling of clays: molecular simulations of the hydration of montmorillonite, Science 271 (1996) 1102–1104.
- [38] R.M. Shroll, D.E. Smith, Molecular dynamics simulations in the grand canonical ensemble: Application to clay mineral swelling, J. Chem. Phys. 111 (1999) 9025–9033.

- [39] D.E. Smith, Y. Wang, H.D. Whitley, Molecular simulations of hydration and swelling in clay minerals, Fluid Phase Equilibria 222 (2004) 189–194.
- [40] N.T. Skipper, F.R.C. Chang, G. Sposito, Monte-Carlo simulation of interlayer molecular-structure in swelling clay-minerals.1. Methodology, Clays Clay Miner. 43 (1995) 285–293.
- [41] N.T. Skipper, G. Sposito, F.R.C. Chang, Monte-Carlo simulation of interlayer molecular-structure in swelling clay-minerals.2. Monolayer hydrates, Clays Clay Miner. 43 (1995) 294–303.
- [42] D.R. Katti, S.R. Schmidt, P. Ghosh, K.S. Katti, Modeling the response of pyrophyllite interlayer to applied stress using steered molecular dynamics, Clays Clay Miner. 53 (2005) 171–178.
- [43] D.R. Katti, K.B. Thapa, K.S. Katti, The role of fluid polarity in the swelling of sodium-montmorillonite clay: a molecular dynamics and Fourier transform infrared spectroscopy study, J. Rock. Mech. Geotech. Eng. 10 (2018) 1133–1144.
- [44] K.B. Thapa, K.S. Katti, D.R. Katti, Compression of Na-montmorillonite swelling clay interlayer is influenced by fluid polarity: a steered molecular dynamics study, Langmuir 36 (2020) 11742–11753.
- [45] S. Ghazanfari, H.M.N. Faisal, K.S. Katti, D.R. Katti, W. Xia, A coarse-grained model for the mechanical behavior of Na-montmorillonite clay, Langmuir (2022).
- [46] K.B. Thapa, K.S. Katti, D.R. Katti, Influence of the fluid polarity on shear strength of sodium montmorillonite clay: a steered molecular dynamics study, Comput. Geotech. 158 (2023) 105398.
- [47] X.-y Ma, L.-f Zhu, X. Zou, X. Kang, Investigation of the interface stick-slip friction behavior of clay nanoplatelets by molecular dynamics simulations, Colloids Surf. A: Physicochem. Eng. Asp. 679 (2023) 132601.
- [48] M. Rahromostaqim, M. Sahimi, Molecular dynamics simulation of hydration and swelling of mixed-layer clays, J. Phys. Chem. C 122 (2018) 14631–14639.
- [49] L. Sun, J.T. Tanskanen, J.T. Hirvi, S. Kasa, T. Schatz, T.A. Pakkanen, Molecular dynamics study of montmorillonite crystalline swelling: roles of interlayer cation species and water content, Chem. Phys. 455 (2015) 23–31.
- [50] L. Tao, X.-F. Tian, Z. Yu, G. Tao, Swelling of K+, Na+ and Ca2+-montmorillonites and hydration of interlayer cations: a molecular dynamics simulation, Chin. Phys. B 19 (2010).
- [51] X. Liu, R. Zhu, J. Ma, F. Ge, Y. Xu, Y. Liu, Molecular dynamics simulation study of benzene adsorption to montmorillonite: Influence of the hydration status, Colloids Surf. A: Physicochem. Eng. Asp. 434 (2013) 200–206.
- [52] A.K. Narayanan Nair, R. Cui, S. Sun, Overview of the adsorption and transport properties of water, ions, carbon dioxide, and methane in swelling clays, ACS Earth Space Chem. 5 (2021) 2599–2611.
- [53] B.J. Teppen, K. Rasmussen, P.M. Bertsch, D.M. Miller, L. Schafer, Molecular dynamics modeling of clay minerals.1. Gibbsite, kaolinite, pyrophyllite, and beidellite, J. Phys. Chem. B 101 (1997) 1579–1587.
- [54] S.R. Schmidt, D.R. Katti, P. Ghosh, K.S. Katti, Evolution of mechanical response of sodium montmorillonite interlayer with increasing hydration by molecular dynamics, Langmuir 21 (2005) 8069–8076.
- [55] H. Heinz, H. Koerner, K.L. Anderson, R.A. Vaia, B.L. Farmer, Force field for micatype silicates and dynamics of octadecylammonium chains grafted to montmorillonite, Chem. Mater. 17 (2005) 5658–5669.
- [56] D.R. Katti, P. Ghosh, S. Schmidt, K.S. Katti, Mechanical properties of the sodium montmorillonite interlayer intercalated with amino acids, Biomacromolecules 6 (2005) 3276–3282.
- [57] K.S. Katti, D. Sikdar, D.R. Katti, P. Ghosh, D. Verma, Molecular interactions in intercalated organically modified clay and clay-polycaprolactam nanocomposites: experiments and modeling, Polymer 47 (2006) 403–414.
- [58] J.C. Phillips, R. Braun, W. Wang, J. Gumbart, E. Tajkhorshid, E. Villa, C. Chipot, R. D. Skeel, L. Kale, K. Schulten, Scalable molecular dynamics with NAMD, J. Comput. Chem. 26 (2005) 1781–1802.
- [59] P.M. Amarasinghe, K.S. Katti, D.R. Katti, Insight into role of clay-fluid molecular interactions on permeability and consolidation behavior of Na-montmorillonite swelling clay, J. Geotech. Geoenviron. Eng. 138 (2012) 138–146.
- [60] R. Shahriyari, A. Khosravi, A. Ahmadzadeh, Nanoscale simulation of Na-Montmorillonite hydrate under basin conditions, application of CLAYFF force field in parallel GCMC, Mol. Phys. 111 (2013) 3156–3167.
- [61] Y.-C. Li, S.-J. Wei, N. Xu, Y. He, Internal forces within the layered structure of Namontmorillonite hydrates: molecular dynamics simulation, J. Phys. Chem. C 124 (2020) 25557–25567.
- [62] H. Zhou, M. Chen, R. Zhu, X. Lu, J. Zhu, H. He, Coupling between clay swelling/ collapse and cationic partition, Geochim. Cosmochim. Acta 285 (2020) 78–99.
- [63] H. Zhao, H. Cui, S. Jiang, W. Awadalseed, J. Guo, W. Yang, X. Kang, Tensile and compressive behavior of Na-, K-, Ca-Montmorillonite and temperature effects, Chem. Phys. 569 (2023) 111855.
- [64] J.F. Xu, T.T. Gu, W.L. Shen, X. Wang, Y. Ma, L. Peng, X. Li, Influence simulation of inorganic salts on montmorillonite elastic mechanical parameters and experimental study, J. China Univ. Pet. 40 (2016) 83–90.
- [65] H. Zhou, M. Chen, R. Zhu, J. Zhu, H. He, How clay delamination supports aseismic slip, Am. Mineral. 108 (2023) 87–99.